



Machine Learning Approaches for Brain Disease Diagnosis: Principles and Recent Advances

Dr.A.S.Shanthi¹, R.Kokila², D. Ananthi³, G. Indhumathi⁴, G. Shobika Sree Malya⁵, S R.Vahini⁶
^{1,2,3,4,5,6} Department of Computer Science And Engineering, Tamilnadu College of Engineering, Tamilnadu, India.

How to cite this paper: Dr.A.S.Shanthi¹, R.Kokila², D. Ananthi³, G. Indhumathi⁴, G. Shobika Sree Malya⁵, S R.Vahini⁶, "Machine Learning Approaches for Brain Disease Diagnosis: Principles and Recent Advances", IJIREE-V3I05-57-60.

Copyright © 2022 by author(s) and 5th Dimension Research Publication.

This work is licensed under the Creative Commons Attribution International License (CC BY 4.0): <http://creativecommons.org/licenses/by/4.0/>

Abstract: Purpose Detection and segmentation of a brain tumor such as glioblastoma multi formed in magnetic resonance (MR) images are often challenging due to its intrinsically heterogeneous signal characteristics. A robust segmentation method for brain tumor MRI scans was developed and tested. Methods Simple thresholds and statistical methods are unable to adequately segment the various elements of the GBM, such as local contrast enhancement, necrosis, and edema. Most voxel-based methods cannot achieve satisfactory results in larger data sets, and the methods based on generative or discriminative models have intrinsic limitations during application, such as small sample set learning and transfer. The promises of these two projects were to model the complex interaction of brain and behavior and to understand and diagnose brain diseases by collecting and analyzing large quantities of data. Archiving, analyzing, and sharing the growing neuroimaging datasets posed major challenges. New computational methods and technologies have emerged in the domain of Big Data but have not been fully adapted for use in neuroimaging. In this work, we introduce the current challenges of neuroimaging in a big data context. We review our efforts toward creating a data management system to organize the large-scale fMRI datasets, and present our novel algorithms/methods A new method was developed to overcome these challenges. Multimodal MR images are segmented into super pixels using algorithms to alleviate the sampling issue and to improve the sample representativeness. Next, features were extracted from the super pixels using multi-level Gabor wavelet filters.

I. INTRODUCTION

BRAIN AND TUMOR SEGMENTATION

Combining image segmentation based on statistical classification with a geometric prior has been shown to significantly increase robustness and reproducibility. Using a probabilistic geometric model of sought structures and image registration serves both initialization of probability density functions and definition of spatial constraints. A strong spatial prior, however, prevents segmentation of structures that are not part of the model. In practical applications, we encounter either the presentation of new objects that cannot be modeled with a spatial prior or regional intensity changes of existing structures not explained by the model. Our driving application is the segmentation of brain tissue and tumors from three-dimensional magnetic resonance imaging (MRI). Our goal is a high-quality segmentation of healthy tissue and a precise delineation of tumor boundaries. We present an extension to an existing expectation maximization (EM) segmentation algorithm that modifies a probabilistic brain atlas with an individual subject's information about tumor location obtained from subtraction of post- and pre-contrast MRI. The new method handles various types of pathology, space-occupying mass tumors and infiltrating changes like edema. Preliminary results on five cases presenting tumor types with very different characteristics demonstrate the potential of the new technique for clinical routine use for planning and monitoring in neurosurgery, radiation oncology, and radiology. A geometric prior can be used by atlas-based segmentation, which regards segmentation as a registration problem in which a fully labeled, template MR volume is registered to an unknown dataset.

High dimensional warping results in a one-to-one correspondence between the template and subject images, resulting in a new, automatic segmentation. These methods require elastic registration of images to account for geometrical distortions produced by pathological processes. Such registration remains challenging and is not yet solved for the general case. The combined elastic atlas registration with statistical classification, Elastic registration of a brain atlas helped to mask the brain from surrounding structures. A further step uses distance from brain boundary" as an additional feature to improve separation of clusters in multi-dimensional feature space. Initialization of probability density functions still requires a supervised selection of training regions. The core idea, namely to augment statistical classification with spatial information to account for the overlap of distributions in intensity feature space, is part of the new method presented in this paper. Automatic segmentation of MR images of normal brains by statistical classification, using an atlas prior for initialization and also for geometric constraints. A most recent extension detects brain lesions as outliers and was successfully applied for detection of multiple sclerosis lesions. Brain tumors, however, can't be simply modeled as intensity outliers due to overlapping intensities with normal tissue and/or significant size. We propose a fully automatic method for segmenting MR images presenting tumor and edema, both mass-effect and infiltrating structures. Additionally, tumor and edema classes are

added to the segmentation. The spatial atlas that is used as a prior in the classification is modified to include prior probabilities for tumor and edema. As with the work done by other groups, we focus on a subset of tumors to make the problem tractable. Our method provides a full classification of brain tissue into white matter, grey matter, tumor, and edema. Because the method is fully automatic, its reliability is optimal. We have applied our tumor segmentation framework to five different datasets, including a wide range of tumor types and sizes Fig. 5 shows results for two datasets. Because the tumor class has a strong spatial prior, many small structures, mainly blood vessels, are classified as tumor because they enhance with contrast. Post processing using level set evolution is necessary to get a final segmentation for the tumor [shows the final spatial priors used for classification of the dataset with the additional tumor and edema channels. We have developed a model-based segmentation method for segmenting head MR image datasets with tumors and in ltrating edema.

This is achieved by extending the spatial prior of a statistical normal human brain atlas with individual information derived from the patient's dataset. Thus, we combine the statistical geometric prior with image-specific information for both geometry of newly appearing objects, and probability density functions for healthy tissue and pathology. Applications to five tumor patients with variable tumor appearance demonstrated that the procedure can handle large variation of tumor size, interior texture, and locality. The method provides a good quality of healthy tissue structures and of the pathology, a requirement for surgical planning or image guided surgery. Thus, it goes beyond previous work that focuses on tumor segmentation only. Currently, we are testing the validity of the segmentation system in a validation study that compares resulting tumor structures with repeated manual experts' segmentations, both within and between multiple experts. A preliminary machine versus human rater validation showed an average overlap ratio of > 90% and an average MAD (mean average surface distance) of 0.8mm, which is smaller than the original voxel resolution. In our future work, we will study the issue of deformation of normal anatomy in the presence of space-occupying tumors. Within the range of tumors studied so far, the soft boundaries of the statistical atlas could handle spatial deformation. However, we will develop a scheme for high dimensional warping of multichannel probability data to get an improved match between atlas and patient images.

II. LITERATURE REVIEW

A system for brain tumor volume estimation via MR imaging and fuzzy connectedness - In this work et.al[1]Liu J, Udupa JK, Odhner D, Hackney D, Moonis G has proposed This paper presents a method for the precise, accurate and efficient quantification of brain tumor (glioblastomas) via MRI that can be used routinely in the clinic. Tumor volume is considered useful in evaluating disease progression and response to therapy, and in assessing the need for changes in treatment plans. A non parametric method for automatic correction of intensity non uniformity in MRI data - In this work et.al[2]Sled JG, Zijdenbos AP, Evans AC has proposed A novel approach to correcting for intensity non uniformity in magnetic resonance (MR) data is described that achieves high performance without requiring a model of the tissue classes present. The method has the advantage that it can be applied at an early stage in an automated data analysis, before a tissue model is available. Intensity non- uniformity correction in MRI: Existing methods and their validation - In this work et.al[3] Belaroussi B, Milles J, Carme S, Zhu YM, Benoit- Cattin H has proposed In this paper, we propose an overview of existing methods. We first sort them according to their location in the acquisition/processing pipeline. Sorting is then refined based on the assumptions those methods rely on. Next, we present the validation protocols used to evaluate these different correction schemes both from a qualitative and a quantitative point of view. Finally, availability and usability of the presented methods is discussed.

III.METHODOLOGY

BAT ALGORITHM:

BAT algorithm, well-known for its optimization ability offers a quicker convergence rate when compared to other contemporary optimization techniques, and it is quite good for performing medical image segmentation. The introduction of BAT algorithm has been made by Zhang et al. and it has a unique principle called echolocation, which is an inbred quality possessed by bats. In general, the bats (mammal) have the ability to detect prey and avoid obstacles using the process of echolocation that relates to the ultrasound signal produced by a bat, which is around 16 KHz and it gets reflected on striking/interfering an obstacle or prey. The introduction of BAT algorithm has been made by Zhang et al. and it has a unique principle called echolocation, which is an inbred quality possessed by bats. In general, the bats (mammal) have the ability to detect prey and avoid obstacles using the process of echolocation that relates to the ultrasound signal produced by a bat, which is around 16 KHz and it gets reflected on striking/interfering an obstacle or prey.

AN GREY LEVEL CO-OCCURRENCE MATRIX

(GLCM) Homomorphism classifier, which does not consider interactions in the labels of adjacent data points. Conversely, DRFs and MRFs consider these interactions, but do not have the same appealing generalization properties as Radial Basis Function. This section will review our GREY LEVEL CO-OCCURRENCE MATRIX (GLCM), an extension of RBF that uses a brain tumor framework to model interactions in the labels of adjacent data points.

$$p(y|x) = \frac{1}{Z} \exp\{ \sum_{i \in S} \log(O(y_i, \gamma_i(x))) + \sum_{j \in N} V(y_i, y_j, X) \}$$

Where $\gamma_i(x)$ computes features from the observations x for location i , $O(y_i, \gamma_i(x))$ s an SVM based

Observation-Matching potential, and $V(y_i, y_j, X)$ is the Local- Consistency potential over a pair-wise neighborhood structure, where N_i are the 8 neighbors around location i .

The Observation-Matching function maps from the observations (features) to class labels. We would like to use SVMs for this potential. However, the decision function in SVMs produces a distance value, not a posterior probability suitable for the DRFs' framework. To convert the output of the decision function to a posterior probability. This efficient method minimizes the risk of over fitting and is formulated as follows:

$$O(y_i = 1 | \gamma_i(X)) = \frac{1}{1 + \exp(A X f(\gamma_i(X)) + B)} \quad (5)$$

The parameters A and B are estimated from training data represented as pairs where $\langle f(\gamma_i(x)), t_i \rangle$ is the real-valued SVM response (here, distance to the separator), and t_i denotes a related probability that $y_i = 1$, represented as the relaxed probabilities: $t_i = \frac{N_+ + 1}{N_+ + 2}$ if $y_i = 1$, $t_i = \frac{N_- + 1}{N_- + 2}$ if $y_i = -1$, where N_+ and N_- are the number of positive and negative class instances. Using these training instances, we can solve the following optimization problem to estimate parameters A and B:

$$\min - \sum_{i=1}^n [t_i \log O(t_i, \gamma_i(x)) + (1 - O(t_i, \gamma_i(x)))] \quad (6)$$

Platt [15] used a Leven berg-Marquardt approach that tried to set B to guarantee that the Hessian approximation was invertible. However, dealing with the constant directly can cause problems, especially for unconstrained optimization problems [13]. Hence, we employed Newton's method with backtracking line search for simple and robust estimation. To avoid overflows and underflows of \exp and \log , we reformulated (6) as

$$\min \sum_{i=1}^n [t_i (A X f(\gamma_i(X)) + B) + \log(1 + \exp(-A X f(\gamma_i(x)) - B))] \quad (7)$$

We use a DRF model for Local-Consistency, since we do not want to make the (traditional MRF) assumption that the label interactions are independent of the features. We adopted the following pairwise Local-Consistency potential

$$V(Y_i, Y_j, X) = \gamma_i \gamma_j (v \cdot \phi_{ij}(X)) \quad (8)$$

Where v is the vector of Local-Consistency parameters to be learned, while $\phi_{ij}(x)$ calculates features for sites i and j . DRFs use a ϕ_{ij} that penalizes for high absolute differences in the features. As we are additionally interested in encouraging label continuity, we used the following function that encourages continuity while discouraging discontinuity: $(\max(\gamma(x)))$ denotes the vector of max values of the features):

$$\phi_{ij}(x) = \max(\gamma(x)) - |\gamma_i(x) - \gamma_j(x)| \max(\gamma(x))$$

GREY LEVEL CO-OCCURRENCE MATRIX

(GLCM)s use a sequential learning approach to parameter estimation. This involves first solving the SVM Quadratic Programming problem (3). The resulting decision function is then converted to a posterior probability using the training data and estimated relaxed probabilities. The Local-Consistency parameters are then estimated from the m training pixels from each of the K training images using pseudo likelihood [12]:

$$V = \arg \max_{V} \prod_{i=1}^m \prod_{k=1}^K p(y_i = k | y_{k \in N_t}, X_k | V) \quad (10)$$

We ensure that the log-likelihood is convex by assuming a Gaussian prior over v that is, $p(v|T)$ is a Gaussian distribution with 0 means and T^{-1} variance (see [9]). Thus, the local consistency parameters are estimated using its log likelihood

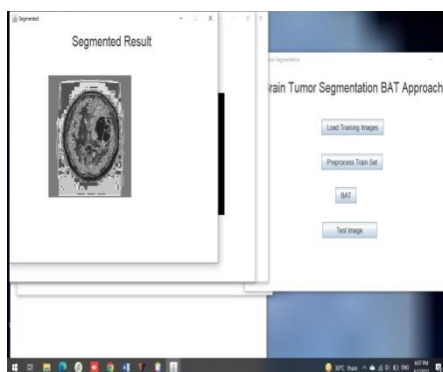
$$\hat{v} = \arg \max_v \sum_{i=1}^m \sum_{k=1}^K \{ O_i(n) + \sum_{j \in N_t} V(\gamma_i(j), \gamma_j(k), X_k) - \log(z_i(k)) \} - \frac{1}{2} T v^T v$$

We used the Jaccard similarity measure to assess the classifications in terms of true positives (p), false positives (fp), and false negatives

$$J = \frac{tp}{tp + fp + fn}$$

IV. RESULTS AND DISCUSSION

We use super pixel-based appearance models to reduce computational cost, improve spatial smoothness, and solve the data sampling problem for training GLCM classifiers on brain tumor segmentation. Also, we develop an affinity model that penalizes spatial discontinuity based on model-level constraints learned from the training data. Finally, our structural denoising based on the symmetry axis and continuity characteristics is shown to remove the false positive regions effectively. The training and validation were performed on high-resolution MR image dataset with augmentations and the result is compared with deep learning bat algorithm model Alex net. The performance of all bat algorithm models is evaluated with the help of performance metrics recall, precision, F score specificity, and overall accuracy.



V.CONCLUSION

Our paper brings together two recent trends in the brain tumor segmentation literature: model-aware similarity and affinity calculations with GREY LEVEL CO-OCCURRENCE MATRIX (GLCM) models with GREY LEVEL CO-OCCURRENCE MATRIX (GLCM)-based evidence terms. In doing so, we make three main contributions. We use super pixel-based appearance models to reduce computational cost, improve spatial smoothness, and solve the data sampling problem for training GREY LEVEL CO-OCCURRENCE MATRIX (GLCM) classifiers on brain tumor segmentation. Also, we develop an affinity model that penalizes spatial discontinuity based on model-level constraints learned from the training data. Finally, our structural denoising based on the symmetry axis and continuity characteristics is shown to remove the false positive regions effectively. Our full system has been thoroughly evaluated on a challenging 20-case GBM and the Bra TS challenge data set and shown to systematically perform on par with the state of the art. The combination of the two tracts of ideas yields better performance, on average, than either alone. In the future, we plan to explore alternative feature and classifier methods, such as classification forests to improve overall performance.

Reference

1. Liu J, Udupa JK, Odhner D, Hackney D, Moonis G (2005) A system for brain tumor volume estimation via MR imaging and fuzzy connectedness. *Comput Med Imaging Graphics* 29(1):21–34
2. Sled JG, Zijdenbos AP, Evans AC (1998) A nonparametric method for automatic correction of intensity nonuniformity in MRI data. *IEEE Trans Med Imaging* 17(1):87–97
3. Belaroussi B, Milles J, Carne S, Zhu YM, Benoit-Cattin H (2006) Intensity non-uniformity correction in MRI: existing methods and their validation. *Med Image Anal* 10(2):234
4. Madabhushi A, Udupa JK (2005) Interplay between intensity standardization and inhomogeneity correction in MR image processing. *IEEE Trans Med Imaging* 24(5):561–57
5. Prastawa M, Bullitt E, Ho S, Gerig G (2004) A brain tumor segmentation framework based on outlier detection. *Med Image Anal* 8(3):275–283
6. Phillips W, Velthuizen R, Phuphanich S, Hall L, Clarke L, Silbiger M (1995) Application of fuzzy c-means segmentation technique for tissue differentiation in MR images of a hemorrhagic glioblastoma multiforme. *Magn Reson Imaging* 13(2):277–290
7. Clark MC, Hall LO, Goldgof DB, Velthuizen R, Murtagh FR, Silbiger MS (1998) Automatic tumor segmentation using knowledge based techniques. *IEEE Trans Med Imaging* 17(2):187–201
8. Fletcher-Heath LM, Hall LO, Goldgof DB, Murtagh FR (2001) Automatic segmentation of non-enhancing brain tumors in magnetic resonance images. *Artif Intell Med* 21(1–3):43–63
9. Warfield SK, Kaus M, Jolesz FA, Kikinis R (2000) Adaptive, template moderated, spatially varying statistical classification. *Med Image Anal* 4(1):43–55
10. Kaus MR, Warfield SK, Nabavi A, Black PM, Jolesz FA, Kikinis R (2001) Automated segmentation of MR images of Brain Tumors I. *Radiology* 218(2):586–591
11. Guillemaud R, Brady M (1997) Estimating the bias field of MR images. *IEEE Trans Med Imaging* 16(3):238–251
12. Corso JJ, Sharon E, Dube S, El-Saden S, Sinha U, Yuille A (2008) Efficient multilevel brain tumor segmentation with integrated bayesian model classification. *IEEE Trans Med Imaging* 27(5):629–640
13. Zhou J, Chan K, Chong V, Krishnan S (2006) Extraction of brain tumor from MR images using one-class support vector machine. In: 27th annual international conference of the engineering in medicine and biology society, 2005. *IEEE-EMBS 2005*. pp 6411–6414
14. Corso J, Yuille A, Sicotte N, Toga A (2007) Detection and segmentation of pathological structures by the extended graph-shifts algorithm. In: *Medical Image Computing and Computer Assisted Intervention—MICCAI*. pp 985–993
15. Schapire RE, Freund Y, Bartlett P, Lee WS (1998) Boosting the margin: a new explanation for the effectiveness of voting methods. *Ann Stat* 26(5):1651–1686